Enantiomeric 4-Acylamino-6-alkyloxy-2 Alkylthiopyrimidines As Potential A_3 Adenosine Receptor Antagonists: HPLC Chiral Resolution and Absolute Configuration Assignment by a Full Set of Chiroptical Spectroscopy

DANIELA ROSSI,[1] RITA NASTI,[1] ANNAMARIA MARRA,[1] SILVIA MENEGHINI,[1,2] GIUSEPPE MAZZEO,[2] GIOVANNA LONGHI,[2] MAURIZIO MEMO,[2] BARBARA COSIMELLI,[3] GIOVANNI GRECO,[3] ETTORE NOVELLINO,[3] FEDERICO DA SETTIMO,[4] CLAUDIA MARTINI,[4] SABRINA TALIANI,[4] SERGIO ABBATE,[2]* AND SIMONA COLLINA[1]**

[1]*Dipartimento di Scienze del Farmaco, Università di Pavia, Pavia, Italy*
[2]*Dipartimento di Medicina Molecolare e Traslazionale, Università di Brescia, Brescia, Italy*
[3]*Dipartimento di Farmacia, Università di Napoli "Federico II", Napoli, Italy*
[4]*Dipartimento di Farmacia, Università di Pisa, Pisa, Italy*

ABSTRACT The chiral separation of enantiomeric couples of three potential A_3 adenosine receptor antagonists: (*R/S*)-N-(6-(1-phenylethoxy)-2-(propylthio)pyrimidin-4-yl)acetamide (**1**), (*R/S*)-N-(2-(1-phenylethylthio)-6-propoxypyrimidin-4-yl)acetamide (**2**), and (*R/S*)-N-(2-(benzylthio)-6-sec-butoxypyrimidin-4-yl)acetamide (**3**) was achieved by high-performance liquid chromatography (HPLC). Three types of chiroptical spectroscopies, namely, optical rotatory dispersion (ORD), electronic circular dichroism (ECD), and vibrational circular dichroism (VCD), were applied to enantiomeric compounds. Through comparison with Density Functional Theory (DFT) calculations, encompassing extensive conformational analysis, full assignment of the absolute configuration (AC) for the three sets of compounds was obtained. *Chirality 28:434–440, 2016.*

KEY WORDS: A_3 adenosine receptor antagonists; chiral HPLC; optical rotatory dispersion (ORD); electronic circular dichroism (ECD); vibrational circular dichroism (VCD); Density Functional Theory (DFT); absolute configuration assignment

In mammals, adenosine acts as a transmitter by binding to four subtypes of G-protein-coupled-receptors (GPCRs), namely, the A_1, A_{2A}, A_{2B}, and the A_3 adenosine receptors (ARs).[1,2] Activation of ARs by agonists, such as adenosine itself or synthetic ligands, leads to different intracellular events starting with inhibition (A_1 and A_3) or stimulation (A_{2A} and A_{2B}) of adenylate cyclase, stimulation of phospholipase C (A_1, A_{2B}, and A_3), activation of potassium channels, and inhibition of calcium channels (A_1).[2] Different from A_1, A_{2A}, and A_{2B} ARs, A_3 AR exhibits significant differences in primary amino acid sequence homology (74%) between human and rat.[3] A_3 AR can be found in human lungs, liver, kidneys, heart, brain, uterus, eyes, and testes,[4] where it is involved in a variety of physiological processes, including cell cycle regulation and cell growth.[5] Given its key role, A_3 AR is considered an attractive target for pharmacological therapies by medicinal chemists.[6,7] A_3 AR agonists may be useful as cardioprotective and cerebroprotective agents, as antiinflammatory and immunosuppressive agents, as cytostatics and chemoprotective compounds in cancer therapy. A_3 AR antagonists might be employed for the acute treatment of stroke, for glaucoma, and also as antiasthmatic and antiallergic drugs. The aforementioned potential clinical applications of A_3 AR ligands have been recently reviewed by Borea et al.[6] Recently, some of us have been involved in the synthesis and biological evaluation of novel classes of antagonists at the human A_3 AR.[8–11] Among those investigated, 4-acylamino-6-alkyloxy-2 alkylthiopyrimidines of general formula **I** stand out for ease of synthesis (Scheme 1), drug likeness, potency, and selectivity for the target receptor.[10] In this class, compounds **Ia** and **Ib** (Scheme 1) exhibit Ki values of 7.5 nM (**Ia**) and 525 nM (**Ib**) towards A_3 AR and excellent selectivity over A_1 and A_{2A} ARs.

Recently, we synthesized the chiral pyrimidines **1-3** (Fig. 1), formally derived from previously reported pyrimidines **Ia** and **Ib** by insertion of a methyl group on the exocyclic carbon atom attached to the oxygen or the sulfur (unpublished results). Specifically, **1** is a methyl derivative of **Ia**, whereas **2** and **3** are methyl derivatives of **Ib**. We reasoned that the new compounds, bearing branched substituents, more lipophilic, and less flexible with respect to their desmethyl counterparts, might be endowed with improved potency and selectivity as A_3 AR antagonists. As a consequence, a stereogenic center is present in compounds **1-3**.

To study the influence of chirality on the putative A_3 AR antagonist properties of structures **1-3**, we performed the chiral resolution of racemic **1-3** and assigned the absolute configuration to pure enantiomers. These tasks were achieved by using chiral high-performance liquid chromatography (HPLC) and chiroptical spectroscopy methods combined with Density Functional Theory (DFT) calculations. In detail, on the basis of our previous experience we resolved enantiomeric **1-3** via enantioselective HPLC on chiral stationary phases (CSPs), this approach being an effective way for both the analytical and the preparative separations of chiral

*Correspondence to: Prof. S. Collina, Dipartimento di Scienze del Farmaco, Università di Pavia, Viale Taramelli 12, 27100 Pavia, Italy. E-mail: simona.collina@unipv.it; S. Abbate, Dipartimento di Medicina Molecolare e Traslazionale, Università di Brescia, Brescia, Italy. E-mail: sergio.abbate@unibs.it
Received for publication 4 December 2015; Accepted 1 March 2016
DOI: 10.1002/chir.22599
Published online 20 April 2016 in Wiley Online Library (wileyonlinelibrary.com).

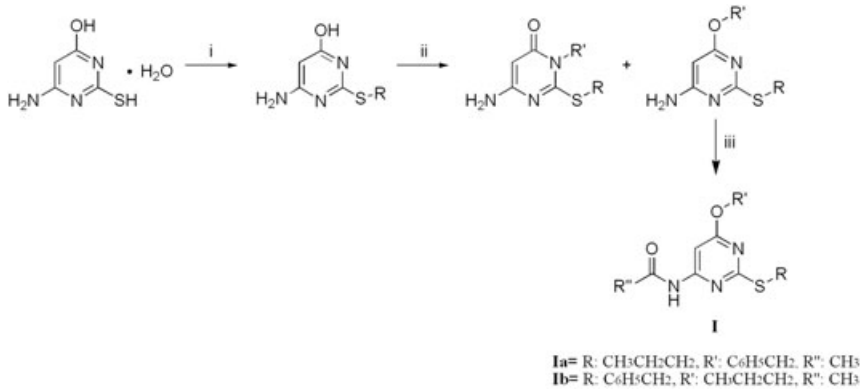

Scheme 1. Synthesis of 4-acylamino-6-alkyloxy-2-alkylthiopyrimidines (**I**). Reagents and conditions: (i)methyl iodide or (phenyl)alkylbromide, NaOH 1M; (ii) methyl iodide or (substituted-phenyl)alkyl bromide, anhydrous DMF, excess K_2CO_3; (iii) acetic or propionic anhydride, catalytic conc. H_2SO_4.

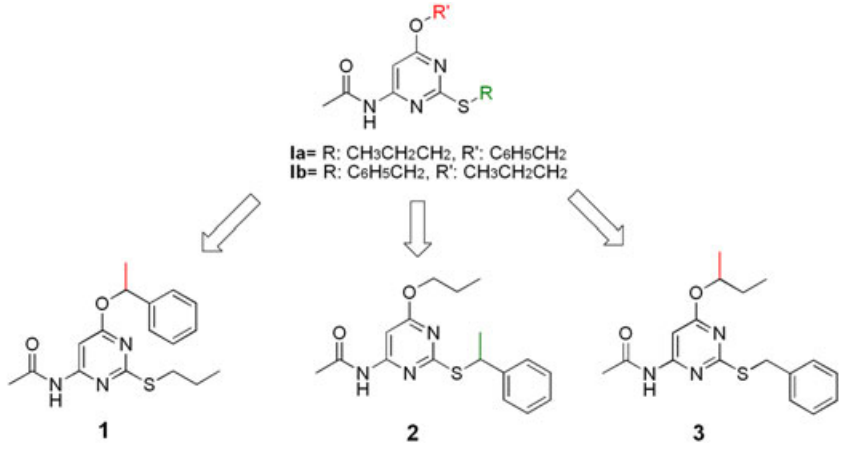

Fig. 1. Structures of the compounds studied in this work.

compounds.[12–14] We carried out the absolute configuration (AC) assignment study of **1-3** resolved enantiomers by a full set of chiroptical spectroscopies and comparison with calculated spectra obtained by ab initio methods (DFT-).[15–17] Thus, optical rotatory dispersion (ORD), electronic circular dichroism (ECD), and vibrational circular dichroism (VCD) spectra were recorded and compared to the calculated ones. The combined use of the three techniques is particularly advised for the AC assigned of flexible molecules, like drugs and natural products, which had been treated previously by the use of separate forms of chiroptical methods.[18–30] Overall, this article describes the work carried out to separate the enantiomeric couples for **1-3** and to assign their absolute configurations in order to understand how chirality may influence their interaction with human A_3 AR.

MATERIALS AND METHODS

Chiral Chromatographic Resolution

Chromatographic resolution was carried out at room temperature on a Jasco (Tokyo, Japan) system consisting of a PU-1580 pump, 851-AS autosampler, and MD-1510 Photo Diode Array (PDA) detector. In order to identify the best conditions to be properly scaled up, analytical screening was performed on the following columns: Chiralpak AD (250 mm × 4.6 mm, 5 μm), Chiralpak AS-H (250 mm × 4.6 mm, 5 μm), Chiralcel OD-H (150 mm × 4.6, 5 μm), and Chiralcel OJ-H (150 mm × 4.6 mm, 5 μm) from Daicel Chemical Industries (Tokyo, Japan). The chiral stationary phases of these columns were amylose tris (3,5-dimethyl-phenylcarbamate), amylose tris[(*S*)-α-methylbenzylcarbamate], cellulose tris(3,5-dimethylphenyl carbamate), and cellulose tris-(4-methylbenzoate), respectively. A Hamilton (Reno, NV) syringe (syringe volume: 2.5 mL; loop: 2 mL) was employed for (semi)-preparative chiral resolutions. Chromatogram acquisitions and elaborations were performed using the Borwin PDA and Borwin Chromatograph software.

Compound Characterization

Optical rotation values were measured on a Jasco photoelectric polarimeter DIP 1000 using a 0.5 dm cell and a sodium and mercury lamp (λ = 589 nm, 435 nm, 405 nm); sample concentration values (c) are given in 10^{-2}g mL^{-1}. Optical data are reported in Supplementary Table SI-2.

Nuclear magnetic resonance spectra were recorded on a Varian (Palo Alto, CA) Inova 500 spectrometer operating at 500 MHz for the proton and 125 MHz for the carbon (compound **1**) or on a Varian Mercury 400 spectrometer operating at 400 MHz for the proton and 100 MHz for the carbon (compounds **2** and **3**) in DMSO-d_6 solution.

*(+)-R-N-[6-(1-Phenylethoxy)-2-(propylsulfanyl)pyrimidin-4-yl]acetamide [(+)-R-**1**]:* ^{1}H-NMR: 10.70 (bs, 1H, NH); 7.39–7.32 (m, 5H, H-Ar); 7.14 (s, 1H, H-5); 6.12 (q, 1H, J = 6.2, OCH) 2.96 (m, 2H, SCH_2); 2.07 (s, 3H, CH_3); 1.60-1.54 (m, 5H, CH_2 and CH_3); 0.94 (t, 3H, J = 7.3, CH_3).^{13}C-NMR: 170.5; 169.6; 169.1; 158.7; 142.3; 128.4; 125.6; 89.8; 73.9; 31.7; 24.0; 24.0; 22.8; 22.4; 13.2.

*(-)-S-N-[6-(1-Phenylethoxy)-2-(propylsulfanyl)pyrimidin-4-yl]acetamide [(-)-S-**1**]:* the ^{1}H-NMR spectrum is identical to that of the corresponding enantiomer.

*(+)-R-N-{2-[(1-Phenylethyl)sulfanyl]-6-propoxypyrimidin-4-yl}acetamide [(+)-R-**2**]:* ^{1}H-NMR: 10.73 (bs, 1H, NH); 7.48–7.44 (m, 2H, H-Ar); 7.36-7.31 (m, 2H, H-Ar); 7.27-7.23 (m, 1H, H-Ar); 7.08 (s, 1H, H-5); 5.00 (q,

1H, J = 7.1, SCH); 4.29–4.17 (m, 2H, OCH_2); 2.09 (s, 3H, CH_3); 1.72-1.62 (m, 5H, CH_2 and CH_3); 0.94 (t, 3H, J = 7.4, CH_3). ^{13}C-NMR: 170.5; 170.0; 169.1; 158.6; 143.0; 128.5; 127.2; 127.1; 89.5; 68.0; 43.5; 24.1; 22.3; 21.6; 10.3.

*(-)-S-N-{2-[(1-Phenylethyl)sulfanyl]-6-propoxypyrimidin-4-yl}acetamide [(-)-S-**2**]:* the ^{1}H-NMR spectrum is identical to that of the corresponding enantiomer.

*(+)-R-N-[2-(Benzylsulfanyl)-6-(butan-2-yloxy)pyrimidin-4-yl]acetamide [(+)-R-**3**]:* ^{1}H-NMR: 10.73 (bs, 1H, NH); 7.44–7.41 (m, 2H, H-Ar); 7.34–7.29 (m, 2H, H-Ar); 7.27-7.24 (m, 1H, H-Ar); 7.07 (s, 1H, H-5); 5.15-5.06 (m, 1H, OCH); 4.39 (s, 2H, SCH_2); 2.09 (s, 3H, CH_3); 1.70-1.52 (m, 2H, CH_2); 1.22 (d, 3H, J = 6.2, CH_3); 0.86 (t, 3H, J = 7.4, CH_3). ^{13}C-NMR: 170,5; 169.7; 169.1; 158.6; 137.9; 128.7; 128.4; 127.0; 89.9; 73.8; 33.9; 28.2; 24.1; 19.1; 9.5.

*(-)-S-N-[2-(Benzylsulfanyl)-6-(butan-2-yloxy)pyrimidin-4-yl]acetamide [(-)-S-**3**]:* the ^{1}H-NMR spectrum is identical to that of the corresponding enantiomer.

ORD Curves, ECD, and VCD Spectra

The DIP 1000-type photoelectric polarimeter from Jasco was used for [α] measurements, which were carried out at room temperature using sodium and mercury sources at three different wavelengths (589, 435, 405 nm) and CG3-50 cell (3.5 mm I.D. × 50 mm pathlength). ORD values were recorded both in chloroform and in methanol for **2** and **3** and just in methanol for **1**. In all cases ORD measurements were carried out for the first eluted enantiomer at all available wavelengths. The ORD and samples concentration values are reported in Table SI-2.

UV and ECD spectra were obtained with a Jasco 815SE apparatus in the range 350–180 nm, using 0.1 mm pathlength quartz cuvettes under the following conditions: 0.5 s integration time, 200 nm/min scan speed, 1 nm bandpass, 10 accumulations. UV/ECD spectra were recorded in acetonitrile for all samples ($2.4 \cdot 10^{-3}$ M and $3.6 \cdot 10^{-3}$ M for **1**, first eluted and second eluted enantiomers respectively; $3.02 \cdot 10^{-3}$ M and $3.32 \cdot 10^{-3}$ M for **2**, first eluted and second eluted enantiomer respectively; for **3** no reliable UV/ECD spectrum was taken, for paucity of compounds).

IR and VCD spectra were collected in the range from 2000 to 850 cm^{-1} with a Jasco FVS6000 FTIR instrument equipped with a liquid N_2-cooled MCT detector. A 200 μm pathlength BaF_2 cell was used with the following conditions: 2000 accumulations, 4 cm^{-1} resolution. IR/VCD spectra were recorded in CCl_4 solution for **2** and **3** (0.068 M and 0.070 M for **2**, first eluted and second eluted compound, respectively; for **3** no reliable VCD data were recorded, see above) and in deuterated methanol solution for **1** (0.040 M both eluted compounds).

Computational Detail

Preliminary conformational analysis was performed for (*R*)-**1-3** with the MMFF94s molecular mechanics (MM) force field: 44 conformers for **1**, 55 for **2** and 43 for **3** were found below 10 Kcal/mol. These sets of conformers were fully optimized at the B3LYP/6-31G* level using the Gaussian09 package.[31] Conformers within 2 kcal/mol in relative free energy with respect to the most stable one were treated at the B3LYP/TZVP level of theory. Calculated free energies were used to determine the Boltzmann population factor of the conformers at 298.15 K.

VCD spectra were calculated for **1** and **2** at the same B3LYP/TZVP level. The IEF-PCM approach was also employed in order to optimize and calculate VCD spectra of deuterated species of **1** (in N-H bond) in CD_3OD solution. For **2** no deuteration was adopted. Calculations of ORD and ECD spectra were performed by the TD-DFT approach with allowance of 30 excited states using the Gaussian Coulomb-attenuated CAM-B3LYP functional and aug-cc-pVDZ as basis set. Calculated VCD spectra were simulated with the Gaussian package[31] assigning 8 cm^{-1} Lorentzian bands shape to all vibrational transitions. ECD bands were assumed to have Gaussian line shape with 0.2 eV bandwidth. Theoretical ORD, ECD, and VCD spectra were obtained as weighted averages by the Boltzmann population factors.

RESULTS AND DISCUSSION

Chiral Resolution

The approach we followed for obtaining enantiopure **1-3** is chiral chromatographic resolution (HPLC). This methodology is suitable both for analytical and preparative purposes and is particularly useful in the early stage of the drug discovery processes, when small-scale separation is needed and both enantiomers have to be investigated.

As there is currently no way to predict which column–mobile phase combination will provide a separation of the desired product, the development process generally involves screening a number of chiral stationary phases and potential mobile phases in a systematic scheme. Based on our experience, for primary HPLC screening we normally use the sets of columns and mobile phases shown in Table SI-1. If this initial screening is not successful, typically we move to a secondary screen, where the lesser-used columns and solvents are employed, again in a similar process. Accordingly, to find a baseline separation quickly, in this work the polysaccharide-based CSPs of Table SI-1 were initially screened. Moreover, the design of the experiments took into account the good solubility of **1-3** in alcohols. For this reason the first set of experiments was performed on the considered columns, eluting with just methanol.[14]

As a result of a first screening with pure methanol, it was found that Chiralcel OJ-H (4.6 mm × 150 mm, 5 μm) lead to relatively short retention times, high enantioselectivity, and high resolution for compound **2** (α = 3.3, R_s = 6.7) and **3** (α = 1.9, R_s = 4.1). Accordingly, these experimental conditions were selected for the scale-up to (semi)-preparative scale. As regards compound **1**, a very poor resolution was obtained (α = 1.33, R_s = 0.3) and therefore it was necessary to extend the screening also to different mobile phases (Table SI-3). Baseline separation, high enantioselectivity, and resolution were obtained eluting with heptane/ethanol 95/5 (v/v) (α = 1.5, R_s = 2.4). Chromatographic profiles of racemates, together with experimental conditions, are given in Fig. 2 and Table 1.

The developed analytical methods were suitably transferred to the semipreparative scale, employing a Chiralcel OJ-H column (10 mm x 250 mm, 5 μm). In this way batches of about 40 mg of racemic **1-2** and of 25 mg of racemic **3** were processed, affording enantiomeric **1-3** in good overall yields (81.8%, 93.1%, and 97.2%, respectively) (Fig. SI-1). The optical rotatory power of the obtained enantiomers, their enantiomeric excess, determined by HPLC and recovery yields are summarized in Table 2. To assign the absolute configuration of the enantiomers of **1-3** we performed ORD analysis and for **1** and **2** we recorded ECD and VCD spectra. The identity of the resolved enantiomers **1-3** was confirmed by ^{1}H-NMR analysis.

Analysis of ORD Data

Let us begin our analysis from compound **2**, which was revealed to be simple to interpret from the computational point of view. The 13 calculated conformers of (*R*)-**2** with population factors above 2% exhibit positive OR values at three different wavelengths and show the same ORD trend (see Fig. SI-2, middle panel). The weighted average theoretical ORD curve shows the same magnitude, but opposite sign as compared with the measured curves of the first eluted enantiomer (Fig. 3, middle panel). From this we deduce that the second eluted enantiomer has (*R*)-AC. Unlike for **2**, the calculated

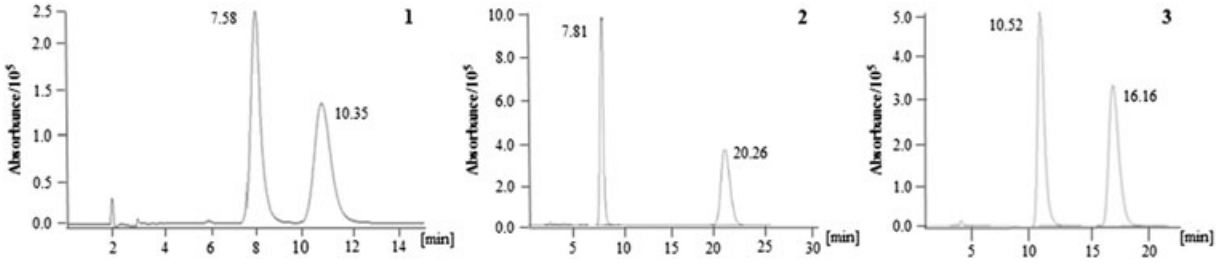

Fig. 2. Analytical chromatographic profiles for (R/S)-1, (R/S)-2, and (R/S)-3 (from left to right) obtained with Chiralcel OJ-H (4.6 mm × 150 mm, 5 μm); eluent heptane/ethanol 95/5 (v/v) for **1** and 100% MeOH for **2** and **3**; flow rate: 1 mL/min; conc.: 1 mg/mL; injection volume: 10 μL; detection at 250, 240, and 254 nm, respectively.

TABLE 1. (Semi)-preparative resolution of racemic 1-3 on a Chiralcel OJ-H column (10 mm x 250 mm, 5 μm)

Compound	Eluent	t_A (min)	t_B (min)	Amount processed (mg)	Concentration (mg/mL)	Number of cycles
1	*n*-heptane/EtOH (95:5 v/v)	13.87	20.25	38	2.0	10
2	MeOH	12.24	32.32	40	5.0	4
3	MeOH	12.79	22.15	25	5.0	3

Flow rate: 4.0 mL/min; injection volume: 2.0 mL.

TABLE 2. Chiroptical characteristics (OR, *ee*, and amount) of the separated enantiomers for 1-3

Compound	λ	C	$[a]_\lambda^{22}$ (MeOH)	*ee*[a]	Isolated amount(mg)	Yield (%)
(+)-1	435	0.1%	+40.4	99.9%[b]	15.2	40.0
(-)-1	435	0.1%	-40.4	99.9%[b]	15.9	41.8
(+)-2	589	0.2%	-214.7	99.9%[c]	18.5	46.3
(-)-2	589	0.2%	+214	99.9%[c]	18.7	46.8
(+)-3	435	0.5%	+56.2	99.9%[c]	12.0	48.0
(-)-3	435	0.5%	-56.4	99.9%[c]	12.3	49.2

[a]Determined on Chiralcel OJ-H (4.6 mm x 150 mm, dp 5 μm) and eluting with
[b]n-heptane 95/5 EtOH (v/v) or
[c]100% methanol.

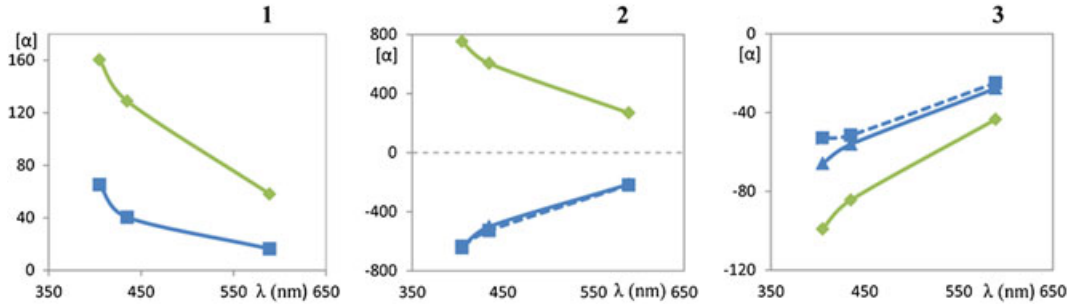

Fig. 3. Comparison of average calculated (CAM-B3LYP/aug-cc-pVDZ on DFT/B3LYP/TZVP input geometries) ORD curves for (R)-**1**-**3** (green line) and experimental (solid blue line, methanol, and dotted blue line, chloroform) for the first eluted couple of compounds **1**-**3**. In the calculated (R)-**3** ORD curve average the conformer in Figure SI-3 is excluded (see text and Fig. SI-2).

(*R*)-**1** ORD curves do not present the same sign and trend for the 15 conformers above 3% population (Fig. SI-2, left panel); the calculated values appear a bit too large with respect to experiments. Anyway, the weighted average calculated ORD curve matches the trend and the sign of the experimental one, which indicates that the first eluted enantiomer has (*R*)-AC (Fig. 3, left panel). Figure SI-2 shows that for good prediction of the ORD curves all calculated conformers are necessary, even those with the wrong sign. For (*R*)-**3**, we noticed that the ORD curves of the 15 calculated conformers with population above 0.8% (Fig. SI-2, right panel) present the same trend except for one of them reported in Figure SI-3 (conformer **3** g).

Even if its population factor is rather low (4.4%), the calculated values of [α] at three λ are very high; so this conformer negatively influences the trend of the average calculated ORD curve. If conformer **3** g is removed, the calculated ORD improves considerably as compared to experiment. Such conformer differs from the other ones by the thio-phenyl group being distorted in such a way as to be closer to the central pyrimidine moiety. However, similar to compound **1**, ORD analysis suggests that the first eluted enantiomer of **3** has (*R*)-configuration.

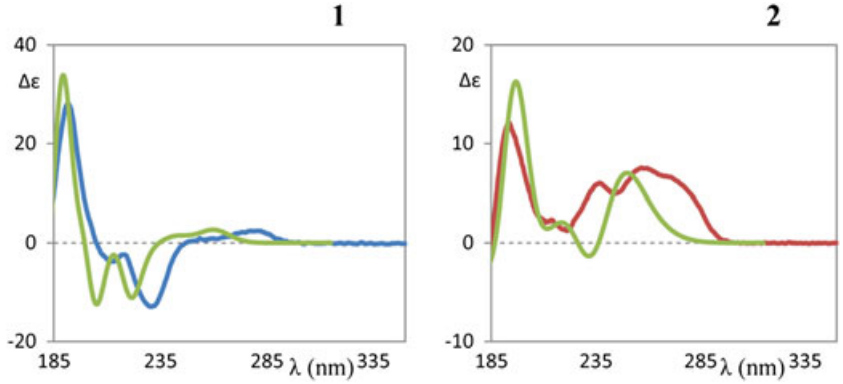

Fig. 4. Comparison of average calculated (CAM-B3LYP on DFT/B3LYP/TZVP input geometries) ECD spectra for (R)-**1**-**2** (green line) and experimental ones (blue line, first eluted, and red line, second eluted).

Analysis of ECD Spectra

Calculated UV absorption spectra of (*R*)-**1** and (*R*)-**2** exhibit five and, respectively, three important bands which nicely correlate with all the experimental ones (Fig. SI-4). For both **1** and **2** the experimental ECD spectra of the two pairs of enantiomers are excellent mirror images of each other (Fig. SI-5): the ECD experimental spectra of **1** and **2** are in good agreement with the calculated average ECD spectra (Fig. 4). Compared to (*R*)-**2**, the ECD spectrum of (*R*)-**1** has the same strong positive 190 nm feature, while the central broad feature at 230 nm is negative in **1**, and positive in **2**. Finally, at about 280 nm, a positive feature is present in both molecules, in **1** being weak and broad, while in **2** being a strong shoulder of a 250 nm band. For **1**, the calculated average ECD spectrum is in good agreement with the experimental one; the small features at high wavelengths are calculated at shorter wavelengths compared to those used for the experiment. For **2,** the situation is slightly worse. To improve the quality of ECD and UV calculated spectra of (*R*)-**2** we applied the PCM model, which allows taking into account the solvent influence. The obtained spectra were similar to the ones calculated in gas phase. Thus, theoretical ECD spectra of (*R*) and (*S*) enantiomers of **1** and **2** are in agreement with the experimental ones of the first eluted enantiomer of **1** and **2,** respectively. These results are in agreement with those obtained performing ORD experiments and therefore the AC was undoubtedly assigned (Fig. 4). In the case of the first eluted enantiomer of **3**, the ECD spectra registered had a poor signal-to-noise ratio and therefore they were not considered.

Analysis of VCD Spectra

Since VCD for compound **1** was run in CD_3OD, where it shows good solubility, we ran a calculation for (*R*)-**1** with N-H replaced by N-D: the average IR calculated spectrum fits rather well the experimental one, especially for the two peaks at ~1565–1544 cm^{-1} and the two peaks at ~1435–1407 cm^{-1} (Fig. 5, left panel). VCD experimental spectra present few

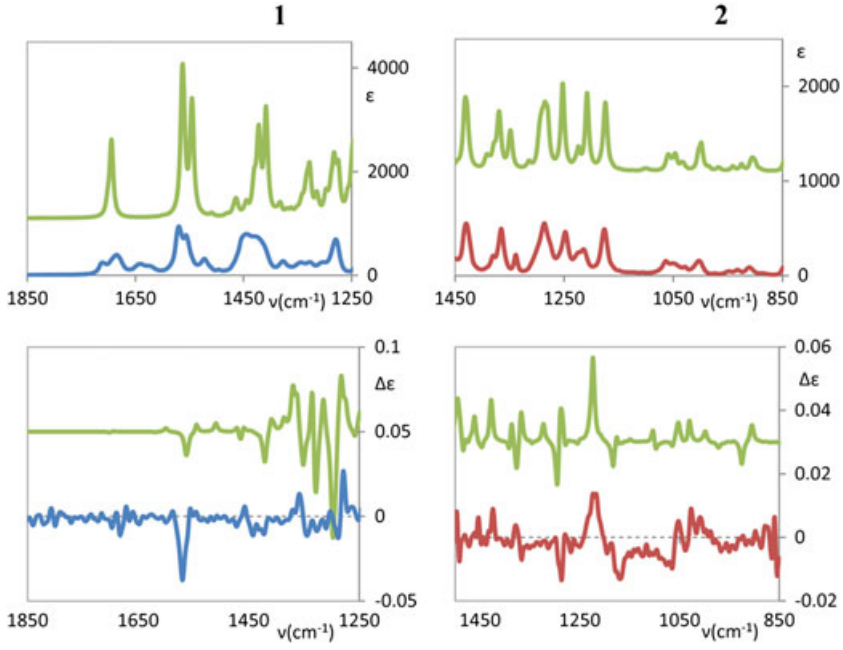

Fig. 5. Comparison of experimental IR and VCD spectra (blue, first eluted enantiomer, and red, second eluted enantiomer) of **1**-**2** with calculated (green) IR and VCD average spectra for (R)-**1**-**2. 1** and **2** experimental spectra are the semi-difference between enantiomers. **1** refers to solution in CD3OD, while data for **2** was taken in CCl_4.

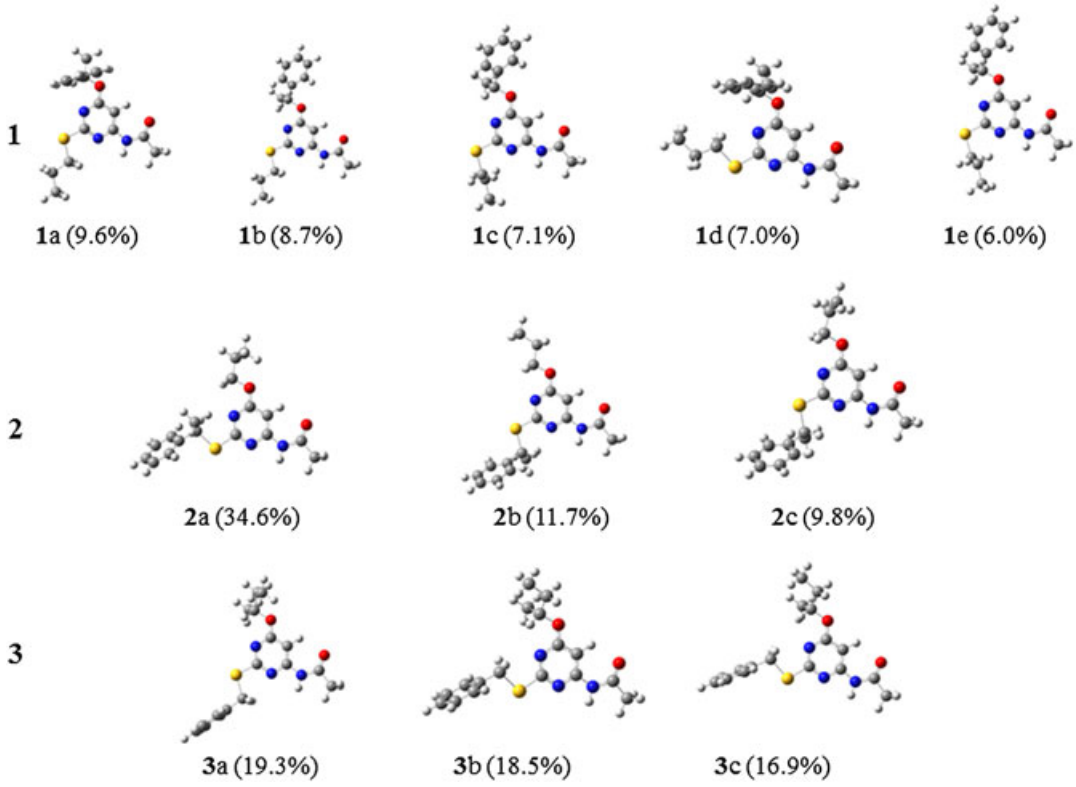

Fig. 6. 3D-structure of the most populated conformers for molecules **1-3** with (R)-configuration calculated in vacuo.

significant bands that are matched by calculations, in sign even if not 100% in magnitude. This may be related to the flexibility of the molecule. The negative VCD band of the first eluted enantiomer, at 1567 cm^{-1}, can be associated with the calculated one at 1558 cm^{-1}, originated by the aromatic C = C and C = N stretching (Fig. 5), while the IR peak around 1693 cm^{-1} can be related to C = O stretching. VCD confirms the same conclusion arrived at by the ORD and ECD techniques. We endeavored to measure IR and VCD spectra of **1** first eluted enantiomer in CCl_4 solution, getting as close as possible to the 0.04 M concentration (**1** is not very soluble in CCl_4). The results are given in Figure SI-6 and a CD_3OD solution, namely, the (*R*)-**1** enantiomer corresponds to the first eluted sample. For **2** the whole IR calculated spectrum provides good prediction of all the experimental peaks, while only few VCD experimental bands appear (Fig. 5, right panel) and are reproduced in sign and magnitude by the average calculated spectra of (*R*)-**2**. Molecular flexibility is so important that the VCD spectrum of one conformer is cancelled by the VCD of another one. The AC is the same predicted by ORD and ECD analyses. This assignment was made on the basis of the first three bands (IR peaks: 1427, 1284, and 1210 cm^{-1}, respectively), which can be attributed to CH_2 wagging (1422 cm^{-1}) and C* bending motions (1285 and 1220 cm^{-1}), respectively. The whole IR spectra is reported in Figure SI-7. The IR and VCD spectra recorded in other solvents ($CDCl_3$ and CS_2) did not give rise to results. Regarding the VCD spectra of (–)-**3**, a poor signal-to-noise ratio was obtained, as already evidenced in the case of ECD spectra.

Conformational Analysis

The previously discussed comparison of experimental and calculated ORD, ECD, and VCD spectra would not have been feasible if a systematic investigation of possible conformers had not been conducted. Indeed, in order to establish AC, one has to carry out a detailed and reliable conformational analysis aimed at understanding the arrangement of the substituents in the different conformers. In Figure 6 we report the five most populated conformers for **1** and the three most populated conformers for **2** and **3** (see also Table SI-4). All investigated conformers present the amide group R" bound to the pyrimidine ring, always in the same position and on the same plane.

CONCLUSION

In the present article we have described the isolation of **1-3** pure enantiomers and the assignment of their absolute configuration in order to investigate the role of chirality on the potential A_3 AR antagonist properties of these compounds. To the best of our knowledge, pharmacological enantioselectivity of A_3 AR antagonists has been previously investigated only by Jacobson and colleagues.[32]

An enantioselective HPLC procedure using a Chiralcel OJ-H column was successfully applied to the enantioresolution of **1-3**, obtaining both enantiomers with an enantiomeric excess of about 99.9% and in amounts suitable for absolute configuration assignment and biological investigation. In line with emerging works, we employed a full set of chiroptical spectroscopies to determine the AC of the resolved enantiomers.[18,25,29] In detail, AC of enantiomeric **1-3** was assigned by comparing experimental and calculated ORD curves and, in the case of enantiomeric **1** and **2**, also comparing ECD and VCD spectra with the DFT calculated ones. It has to be underlined that all the applied techniques gave rise to converging conclusions. However, this behavior is not universal and VCD sometimes

arrives at safer conclusions.[18,25,33] To sum up, the first eluted enantiomers are *(R)*-**1**, *(S)*-**2,** and *(R)*-**3**, and the second eluted ones are *(S)*-**1**, *(R)*-**2,** and *(S)*-**3,** respectively. Overall, this work provided enantiomerically pure **1-3** currently being employed by us to study the influence of chirality on the interaction of this class of compounds with human A_3 AR. The results of these efforts will be reported in due course.

ACKNOWLEDGMENTS

We thank CINECA, via Raffaello Sanzio 4, 20090 Segrate, MI, Italy, for granting us computer time.

SUPPORTING INFORMATION

Additional supporting information may be found in the online version of this article at the publisher's web-site.

LITERATURE CITED

1. Műller CE, Jacobson KA. Recent developments in adenosine receptor ligands and their potential as novel drugs. Biochim Biophys Acta 1808;2011:1290–1308.
2. Fredholm BB, IJzerman AP, Jacobson KA, Linden J, Muller CE. International union of basic and clinical pharmacology. LXXXI. Nomenclature and classification of adenosine receptors-an update. Pharmacol Rev 2011;63:1–34.
3. Salvatore CA, Jacobson MA, Taylor HE, Linden J, Johnson RG. Molecular cloning and characterization of the human A_3 adenosine receptor. Proc Natl Acad Sci U S A 1993;90:10365–10369.
4. Linden J. Cloned adenosine A_3 receptors: Pharmacological properties, species differences and receptor functions. Trends Pharmacol Sci 1994;15:298–306.
5. Brambilla R, Cattabeni F, Ceruti S, Barbieri D, Franceschi C, Kim Y-C, Jacobson KA, Klotz K-N, Lohse MJ, Abbracchio MP. Activation of the A_3 adenosine receptor affects cell cycle progression and cell growth. Naunyn Schmiedeberg's Arch Pharmacol 2000;361:225–234.
6. Borea PA, Varani K, Vincenzi F, Baraldi PG, Tabrizi MA, Merighi S, Gessi S. The A_3 adenosine receptor: history and perspectives. Pharmacol Rev 2015;67:74–102.
7. Müller CE. Medicinal chemistry of adenosine A_3 receptor ligands. Curr Top Med Chem 2003;3:445–62.
8. Novellino E, Cosimelli B, Ehlardo M, Greco G, Iadanza M, Lavecchia A, Rimoli MG, Sala A, Da Settimo A, Primofiore G, Da Settimo F, Taliani S, La Motta C, Klotz K-N, Tuscano D, Trincavelli ML, Martini C. 2-(Benzimidazol-2-yl)quinoxalines: A novel class of selective antagonists at human A_1 and A_3 adenosine receptors designed by 3D database searching. J Med Chem 2005;48:8253–8260.
9. Da Settimo F, Primofiore G, Taliani S, Marini AM, La Motta C, Simorini F, Salerno S, Sergianni V, Tuccinardi T, Martinelli A, Cosimelli B, Greco G, Novellino E, Ciampi O, Trincavelli ML, Martini C. 5-Amino-2-phenyl[1,2,3]triazolo[1,2a][1,2,4]benzotriazin-1-one: a versatile scaffold to obtain potent and selective A_3 adenosine receptor antagonists. J Med Chem 2007;50:5676–5684.
10. Cosimelli B, Greco G, Ehlardo M, Novellino E, Da Settimo F, Taliani S, La Motta C, Bellandi M, Tuccinardi T, Martinelli A, Ciampi O, Trincavelli ML, Martini C. Derivatives of 4-amino-6-hydroxy-2-mercaptopyrimidine as novel, potent, and selective A_3 adenosine receptor antagonists. J Med Chem 2008;51:1764–1770.
11. Taliani S, La Motta C, Mugnaini L, Simorini F, Salerno S, Marini AM, Da Settimo F, Cosconati S, Cosimelli B, Greco G, Limongelli V, Marinelli L, Novellino E, Ciampi O, Daniele S, Trincavelli ML, Martini C. Novel N^2-substituted pyrazolo[3,4-d]pyrimidine adenosine A_3 receptor antagonists: Inhibition of A_3-mediated human glioblastoma cell proliferation. J Med Chem 2010;53:3954–3963.
12. Lien AN, Hua H, Chuong PH. Chiral drugs. an overview. Int J Biomed Sci 2006;2:85–100.
13. Gaggeri R, Rossi D, Collina S, Mannucci B, Baierl M, Juza M. Quick development of an analytical enantioselective high performance liquid chromatography separation and preparative scale-up for the flavonoid Naringenin. J Chrom A 2011;1218:5414–5422.
14. Rossi D, Pedrali A, Marra A, Pignataro L, Schepmann D, Wünsch B, Ye L, Leuner K, Peviani M, Curti D, Azzolina O, Collina S. Studies on the enantiomers of RC-33 as neuroprotective agents: Isolation, configurational assignment, and preliminary biological profile. Chirality 2013;25:814–822.
15. Nafie LA. Vibrational optical activity, principles and applications. New York; John Wiley & Sons: 2011.
16. Polavarapu PL, Zhao C. Vibrational circular dichroism: a new spectroscopic tool for biomolecular structural determination. Fresenius J Anal Chem 2000;366:727–734.
17. Abbate S, Lebon F, Longhi G, Morelli CF, Ubiali D, Speranza G. Vibrational and electronic circular dichroism spectroscopies and DFT calculations for the assignment of the absolute configuration of hydroxysubstituted 2-tetralols. RSC Adv 2012;2:10200–10208.
18. Polavarapu PL. A single chiroptical spectroscopic method may not be able to establish the absolute configurations of diastereomers: dimethylesters of hibiscus and garcinia acids. J Phys Chem A 2011;115:5665–5673.
19. Mazzeo G, Santoro E, Andolfi A, Cimmino A, Troselj P, Petrovic AG, Superchi S, Evidente A, Berova N. Absolute configurations of fungal and plant metabolites by chiroptical methods. ORD, ECD, and VCD studies on phyllostin, scytolide, and oxysporone. J Nat Prod 2013;76:588–599.
20. Scafato P, Caprioli F, Pisani L, Padula D, Santoro F, Mazzeo G, Abbate S, Lebon F, Longhi G. Combined use of three forms of chiroptical spectroscopies in the study of the absolute configuration and conformational properties of 3-phenylcyclopentanone, 3-phenylcyclohexanone, and 3-phenylcycloheptanone. Tetrahedron 2013;69:10752–10762.
21. Górecki M. A configurational and conformational study of (-)-Oseltamivir using a multi-chiroptical approach. Org Biomol Chem 2015;13:2999–3010.
22. Polavarapu PL. Molecular structure determination using chiroptical spectroscopy: where we may go wrong? Chirality 2012;24:909–920.
23. Gordillo-Román B, Camacho-Ruiz J, Bucio MA, Joseph-Nathan P. Vibrational circular dichroism discrimination of diastereomeric cedranol acetates. Chirality 2013;25:939–951.
24. Felippe LG, Batista JM Jr, Baldoqui DC, Nascimento IR, Kato MJ, He Y, Nafie LA, Furlan M. VCD to determine absolute configuration of natural product molecules: secolignans from Peperomia blanda. Org Biomol Chem 2012;10:4208–4214.
25. Abbate S, Longhi G, Castiglioni E, Lebon F, Wood PM, Woo LWL, Potter BVL. Determination of the absolute configuration of aromatase and dual aromatase-sulfatase inhibitors by vibrational and electronic circular dichroism spectra analysis. Chirality 2009;21:802–809.
26. Brittain HG. Application of chiroptical spectroscopy in the characterization of compounds having pharmaceutical importance. In: Berova N, Nakanishi K, Woody RW editors, Circular dichroism principles and application, 2nd ed. New York: Wiley-VCH; 2000. p 819–844.
27. Keiderling TA. Peptide and protein conformational studies with vibrational circular dichroism and related spectroscopies. In: Berova N, Nakanishi K, Woody RW editors, Circular dichroism principles and application, 2nd ed. New York: Wiley-VCH; 2000. p 621–666.
28. Nakahashi A, Miura N, Monde K, Tsukamoto S. Stereochemical studies of hexylitaconic acid, an inhibitor of p53–HDM2 interaction. Bioorg Med Chem Lett 2009;19:3027–3030.
29. He Y, Wang B, Dukor RK, Nafie LA. Determination of absolute configuration of chiral molecules using vibrational optical activity: a review. Appl Spectrosc 2011;65:699–723.
30. Stephens PJ. Vibrational circular dichroism: a new tool for the stereochemical characterization of chiral molecules. In: Bultinck P, De Winter H, Langenaeker W, Tollenaere JP editors, Computational medicinal chemistry for drug discovery. New York: Marcel Dekker; 2005. p 699–726.
31. Gaussian 09, Revision A.02, Frisch MJ, Trucks GW, Schlegel HB, Scuseria GE, Robb MA, Cheeseman JR, Scalmani G, Barone V, Mennucci B, Petersson GA, Nakatsuji H, Caricato M, Li X, Hratchian HP, Izmaylov AF, Bloino J, Zheng G, Sonnenberg JL, Hada M, Ehara M, Toyota K, Fukuda R, Hasegawa J, Ishida M, Nakajima T, Honda Y, Kitao O, Nakai H, Vreven T, Montgomery JA Jr., Peralta JE, Ogliaro F, Bearpark M, Heyd JJ, Brothers E, Kudin KN, Staroverov VN, Kobayashi R, Normand J, Raghavachari K, Rendell A, Burant JC, Iyengar SS, Tomasi J, Cossi M, Rega N, Millam JM, Klene M, Knox JE, Cross JB, Bakken V, Adamo C, Jaramillo J, Gomperts R, Stratmann RE, Yazyev O, Austin AJ, Cammi R, Pomelli C, Ochterski JW, Martin RL, Morokuma K, Zakrzewski VG, Voth GA, Salvador P, Dannenberg S, Dapprich S, Daniels AD, Farkas Ö, Foresman JB, Ortiz JV, Cioslowski J, Fox DJ. Gaussian. Wallingford CT: Gaussian, Inc.; 2009.
32. Jiang J, Li AH, Jang SY, Chang L, Melman N, Moro S, Ji X, Lobkovsky EB, Clardy JC, Jacobson KA. Chiral resolution and stereospecificity of 6-phenyl-4-phenylethynyl-1,4-dihydropyridines as selective A_3 adenosine receptor antagonists. J Med Chem 1999;42:3055–3065.
33. Abbate S, Burgi LF, Castiglioni E, Lebon F, Longhi G, Toscano E, Caccamese S. Assessment of configurational and conformational properties of naringenin by vibrational circular dichroism. Chirality 2009;21:436–441.